Electronic supplementary information

High and Anisotropic Carrier Mobility in Experimentally Possible Ti_2CO_2 (MXene) Monolayer and Nanoribbons

Xu Zhang, Xudong Zhao, Dihua Wu, Yu Jing, Zhen Zhou*

Key Laboratory of Advanced Energy Materials Chemistry (Ministry of Education), Computational Centre for Molecular Science, Institute of New Energy Material Chemistry, Collaborative Innovation Center of Chemical Science and Engineering (Tianjin), School of Materials Science and Engineering, National Institute for Advanced Materials, Nankai University, Tianjin 300071, P. R. China

*Corresponding Author, Email: zhouzhen@nankai.edu.cn (ZZ).

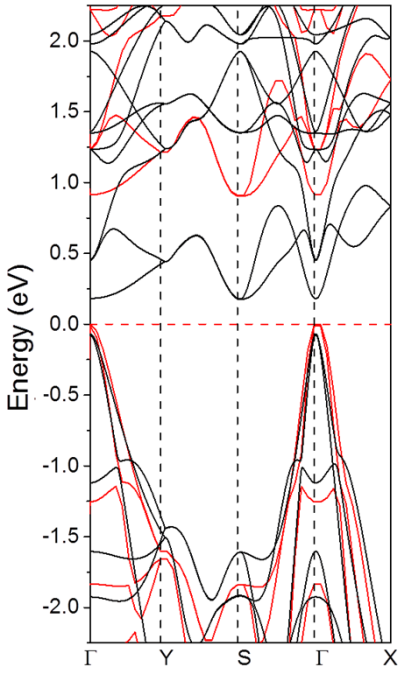

Fig. S1. Band structure near Fermi level calculated with HSE06 functional (red line) and PBE functional (black line) for Ti_2CO_2 monolayer.

Table S1. Effective mass |m*| (m_e) calculated by PBE functional and HSE06 functional.

	PBE |m*| (m_e)	HSE06 |m*| (m_e)
electrons (x)	0.44	0.38
holes (x)	0.14	0.14
electrons (y)	4.53	3.73
holes (y)	0.16	0.20

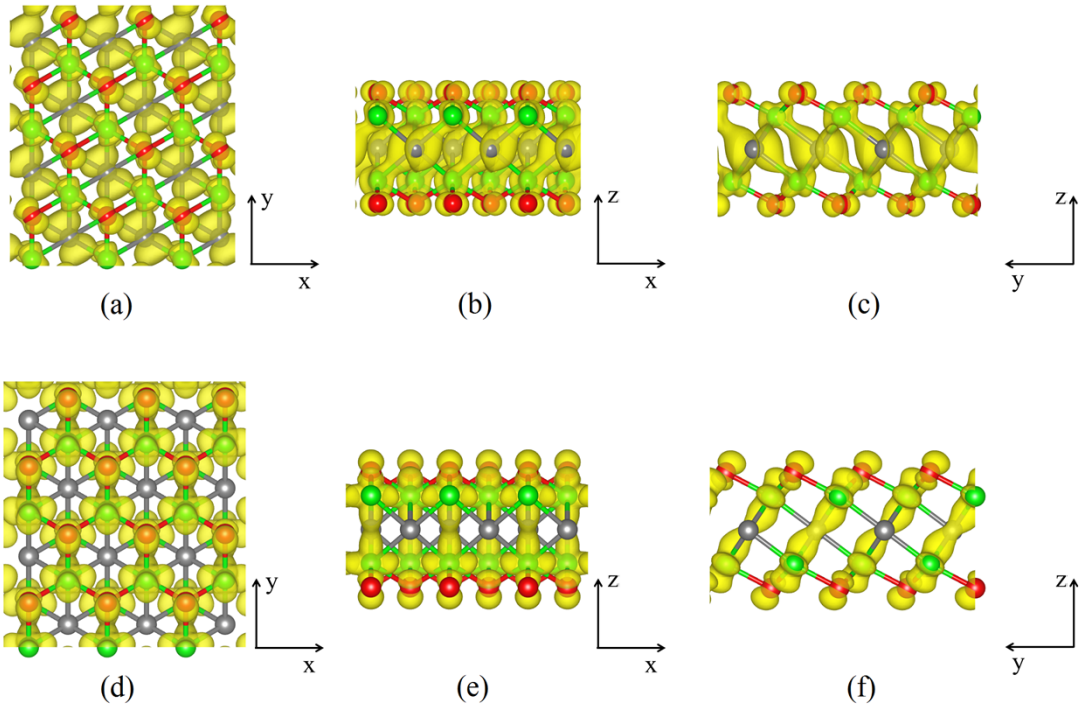

Fig. S2. Spatial structure of wave functions for Ti_2CO_2 monolayer at Γ point using an isosurface of 0.005 e $Å^{-3}$. The top (a) and the side view along x (b) and y (c) direction of VBM. The top (d) and the side view along x (e) and y (f) direction of CBM.

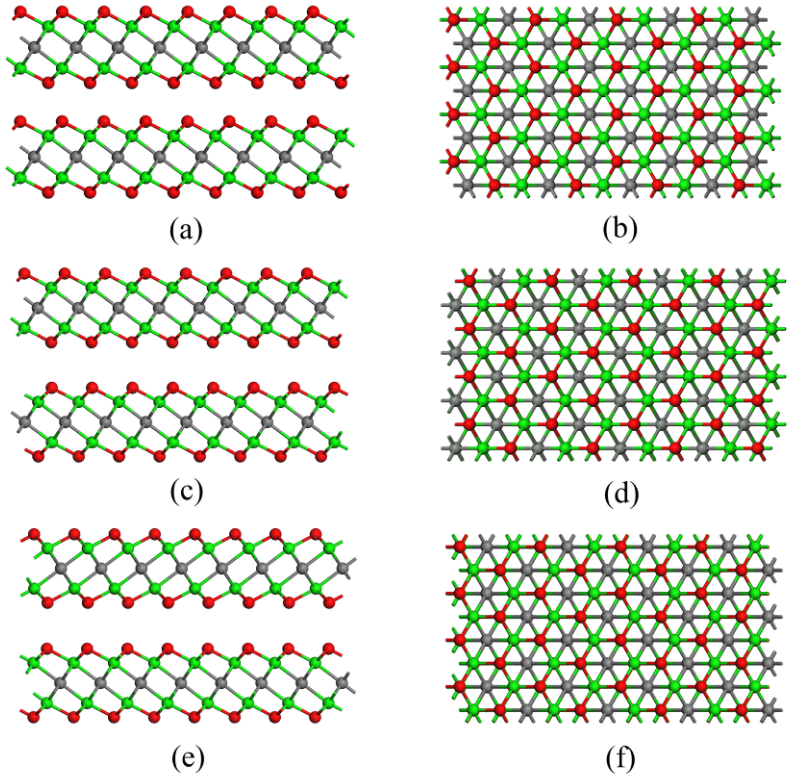

Fig. S3. Optimized geometries of three kinds of Ti_2CO_2 bilayer. (a) Side and (b) top view of structure I; (c) side and (d) top view of structure II; (e) side and (f) top view of structure III.

Three kinds of structures were considered as shown in Fig. S2. Two layers are arranged in the same way are labeled structure I. Like structure I, structure II corresponds to the configuration with the bottom oxygen atoms of the top layer above the top oxygen atoms of the sub layer. Structure III is the configuration with the top layer mirroring the image of the sub layer. After the structure optimization, structure I is the most stable. As a result, the carrier mobility of structure I was calculated and it shown in Table S2.

Table S2. Effective mass |m*| (m_e), in-plane stiffness C (N/m), DP constant $|E_l|$ (eV) and carrier mobility μ ($cm^2\ V^{-1}\ s^{-1}$) for electrons and holes along x and y directions in I Ti_2CO_2 bilayer.

	|m*| (m_e)	C (N/m)	$|E_l|$ (eV)	μ ($cm^2\ V^{-1}\ s^{-1}$)
electrons (x)	0.39	526.48	4.63	2.24×10^3
holes (x)	0.16	526.48	2.02	7.20×10^4
electrons (y)	3.75	527.89	1.44	2.57×10^2
holes (y)	0.16	527.89	3.14	2.87×10^4

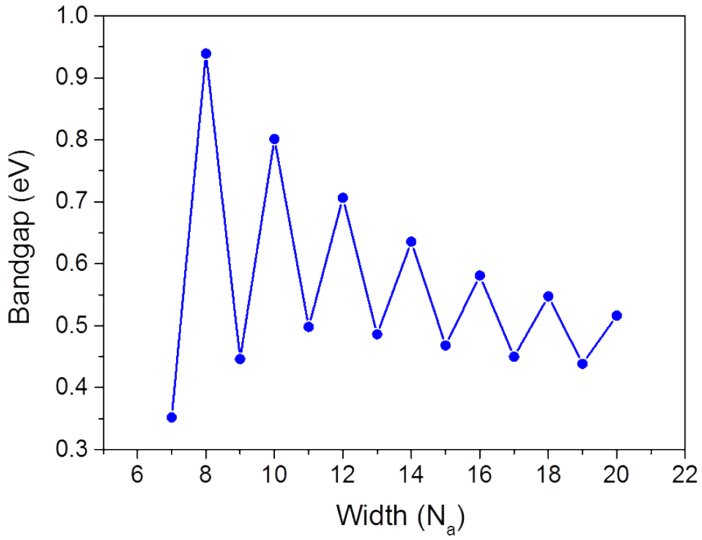

Fig. S4. The variation of band gap with width N_a of armchair nanoribbons.

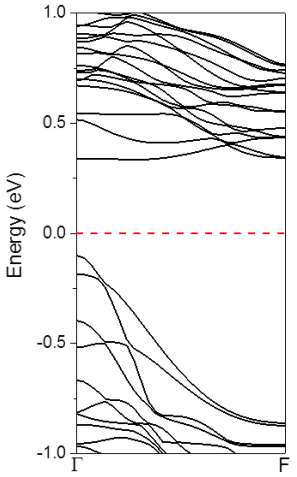

Fig. S5. Band structure near Fermi level for armchair Ti_2CO_2 nanoribbon with N_a=19.

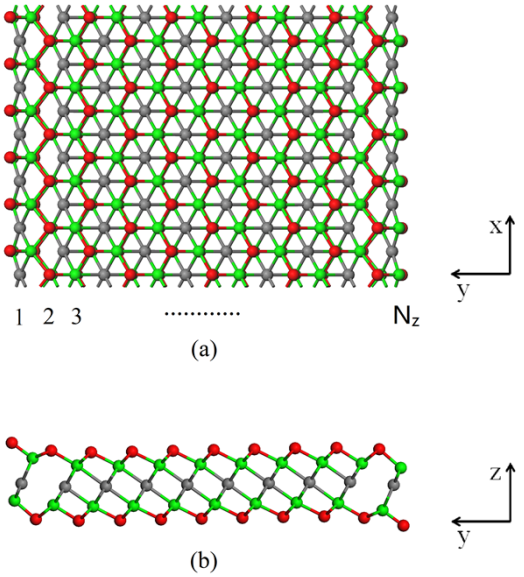

Fig. S6. Optimized geometries of zigzag Ti_2CO_2 nanoribbon. (a) Top view of zigzag Ti_2CO_2 nanoribbon with width N_z=15. (b) Side view of zigzag Ti_2CO_2 nanoribbon.

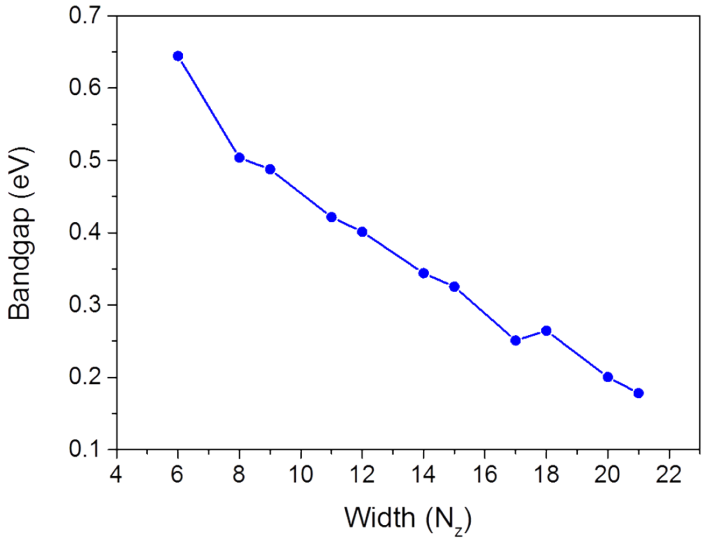

Fig. S7. The variation of band gap with the width N_z of zigzag nanoribbons.

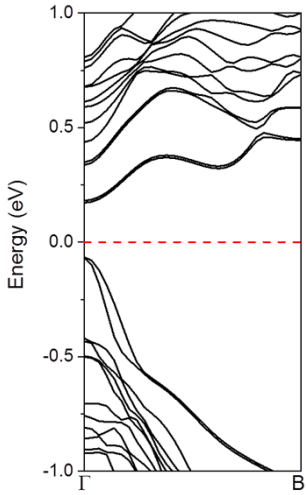

Fig. S8. Band structure near Fermi level for zigzag Ti_2CO_2 nanoribbon with N_z=18.

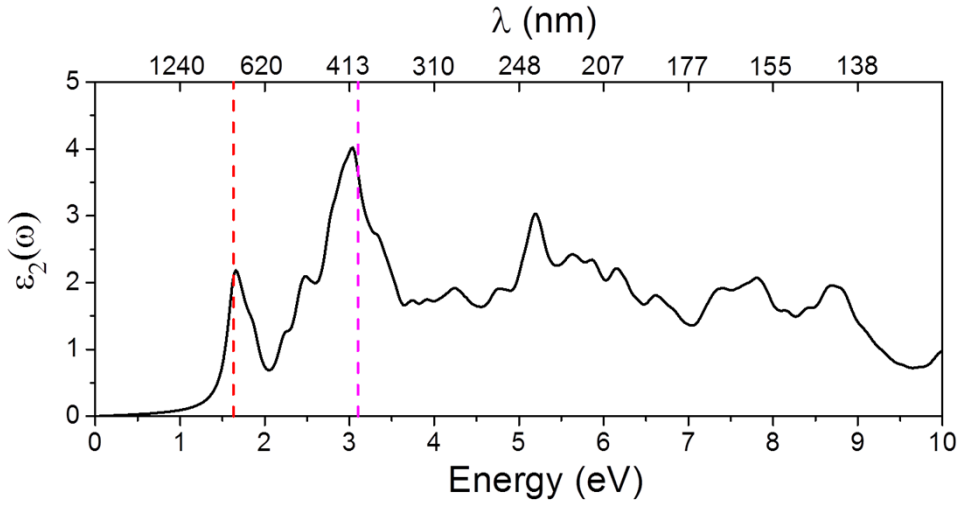

Fig. S9. Imaginary parts $\varepsilon_2(\omega)$ of dielectric function for Ti_2CO_2 monolayer. The area between the red and the purple lines represents the visible range.

The imaginary part $\varepsilon_2(\omega)$ of dielectric function for Ti_2CO_2 monolayer was calculated by HSE06 to investigate the optical absorption. The $\varepsilon_2(\omega)$ terms shown in Fig. S9 are the average of x, y and z direction, that is to say, $\varepsilon_2(\omega) = 1/3(\varepsilon_{xx}(\omega)+\varepsilon_{yy}(\omega)+\varepsilon_{zz}(\omega))$.